



Arsenate adsorption from aqueous solution using iron-loaded *Azadirachta indica* roots: batch and fixed-bed column study

Ghazi Mohd Sawood*, S.K. Gupta

Department of Chemical Engineering, Harcourt Butler Technical University, Kanpur, India, Tel. +91 9918040404; emails: mohdsaud22@gmail.com (G.M. Sawood), skgupta@hbtu.ac.in (S.K. Gupta)

Received 21 October 2019; Accepted 9 June 2020

ABSTRACT

Batch and fixed-bed column studies were carried out to investigate the potential of an economic and eco-friendly adsorbent (iron impregnated *Azadirachta indica* roots (AIR)), for the remediation of arsenate. Maximum adsorption of 96.811% ($q_{e,exp} = 10.586 \mu\text{g/g}$) was obtained at an initial arsenate concentration of 100 $\mu\text{g/L}$, pH of 6.0, adsorbent dose of 1 g/L and contact time of 30 min. The presence of co-existing anions like PO_4^{3-} , SiO_3^{2-} decreases the adsorption capacity whereas cation does not have any effect on the same. Kinetics, isotherms, and thermodynamic studies were also conducted for understating the adsorption process in a better way. The adsorption data fitted best in the Langmuir model ($R^2 = 0.9918$ and $q_{max} = 29.82 \mu\text{g/g}$), which reveals the removal takes place as monolayer adsorption with homogenous energy levels. Adsorption kinetics study reveals that the pseudo-second-order kinetics ($R^2 = 0.9966$, $q_e = 10.2832$) controls the adsorption process. Thermodynamics studies show exothermic and spontaneous adsorption of arsenate on Fe-AIR. In fixed-bed column operations, effects of various operating parameters like bed height, the influent concentration of As(V), flow rate, column diameter were investigated to evaluate the removal efficiency. At optimum experimental conditions ($C_i = 1,000 \mu\text{g/L}$, bed height = 9 cm, flow rate = 3 mL/min, column diameter = 3 cm and pH 7.0), maximum uptake ($q_e = 93.3 \mu\text{g/g}$) with maximum breakthrough (450 min) was achieved. Breakthrough curves were used to analyze the effect of operating parameters on adsorption. Thomas model was used to determine the saturated concentration and the Yoon–Nelson model was applied to determine the required time for 50% adsorbate breakthrough. The present system developed for arsenate remediation is rapid, economic, and reproducible and can be applied to any resource of arsenic-contaminated water. The Fe-AIR fixed column can be regenerated and reused many times. The adsorption capacity decreases to 31.5% after 5 cycles.

Keywords: Arsenate; Fe-AIR; Breakthrough curve; Column operation; Regeneration

1. Introduction

Arsenic in drinking water is considered as a potential threat to human health. It is ranked as the number one carcinogenic substance and listed as number five among potentially toxic elements according to the Comprehensive Environmental Response, Compensation, and Liability act [1]. More than 70 countries, including the United States,

Southeast Asian countries, China, Hungary, Chile, etc. were affected by arsenic contamination [2]. Due to highly toxic nature towards human health, the maximum allowable Arsenic concentration in drinking water has been reduced to 10 from 50 $\mu\text{g/L}$ by the World Health Organization (WHO) [3]. Under different redox situations and pH, arsenic is present in various oxidation states (-3, 0, 3, and 5) in the aquatic system and its chemistry is complicated. Under

* Corresponding author.

oxidizing conditions and in the pH range of 5–7, As(V) is dominating species in the form of HAsO_4^{2-} , HAsO_4^{-1} , and HAsO_4 while under mild reducing conditions, As(III) predominates and exists as $\text{H}_3\text{AsO}_3^{-2}$, $\text{H}_3\text{AsO}_3^{-1}$, or H_3AsO_3 [4]. In human bodies, Arsenate readily reduces to arsenite at low dosages. It is important to treat the total arsenic rather than the distribution of arsenate and arsenite from the contaminated water [5]. Only the conversion of arsenite to arsenate does not reduce arsenic toxicity. Thus it is necessary to develop efficient As(V) removal technologies after pre-oxidation of contaminated water. There are various methods including coagulation and flocculation, membrane filtration, ion exchange, electrochemical precipitation, and adsorption were proposed for the Arsenic remediation from drinking water [6]. It has been reported that along with technical barriers, economic hurdles are also very prominent in arsenic remediation as arsenic-containing groundwater mostly found in developing countries. Therefore, cheaper and technically good methods are required for the treatment of arsenic-contaminated water. Out of the mentioned methods, electrochemical precipitation has the problem of disposal of waste, membrane filtration, and ion exchange technique are less cost-efficient methods [7]. The wide use of the adsorption process is in comparison to other arsenic remediation techniques is due to its simplicity in operation, low cost of operation, and availability [8].

In the recent past, the demand for biosorption and agro-based adsorption processes increased. This hike in the demand can be attributed to the fact that they are relatively very cheap, their bulk abundance, easy regeneration, and generation of minimum sludge. Moreover, this class of adsorbent also tends to form the metal complex of their functional group with metal ions which in turn result in high affinity [9]. Lignin, hydrocarbons of water, hemicellulose, proteins, functional groups of starch are the essential components derived from agro-waste that are responsible for forming a metal complex, which results in sequestering [10].

The powdered form of roots of the *Azadirachta indica* tree is a very good example of non-conventional bio-adsorbent. In the recent past, adsorbents synthesized from bark and leaves of *Azadirachta indica* tree draw the attention of researchers, due to its easy availability across the globe. 90% of As(III) removal at pH 5 was reported using zinc oxide nanoparticle entrenched on leaf extract of *Azadirachta indica* [11]. At 6 pH and 100 $\mu\text{g/L}$ arsenic concentration, 79% of arsenic removal from the groundwater reported using modified bark powder of *Azadirachta indica* [12]. Under optimized experimental conditions (0–500 $\mu\text{g/L}$, pH of 6.5), 89% of As(III) removal achieved using powdered bark of *Azadirachta indica* [13]. Remediation of other pollutants including Zn(II) [14], Cd(II) [15], Cr(VI) [16] and dyes [17] from aqueous solution also investigated using *Azadirachta indica* powder. Earlier the roots of water hyacinth plant (81% arsenic removal at 6.0 pH and 10 mg/L concentration [18], eucalyptus (94% removal at pH = 6.0, $t = 47.5$ min, $C_0 = 2.75$ mg/L and $m = 1.5$ mg/L)), ribwort plantain, lichens, mosses, Chinese brake fern, crowberry, *Tamarix* and many more plants were used for arsenic removal still, not a single research has reported removal of As(V) using roots of *Azadirachta indica* tree.

These findings attributed to great interest in analyzing the possibility for application of [19] powdered roots

of *Azadirachta indica* tree in the remediation of As(V) from aqueous solution. Since the unmodified barks or leaves of *Azadirachta indica* tree has proven to be reasonably significant adsorbents for the removal of As(III) and other pollutants, it is essential to modify the properties of adsorbents to achieve better efficiencies for As(V) removal. Various researches show that iron and its compounds are very effective adsorbents for the remediation of arsenic from water, but due to their fragile nature and the high cost, they cannot be used alone. Many Fe based adsorbents are used for As(III) removal [19–23] but very few such adsorbents were used for As(V) remediation [24,25]. In the present study, surface modification of *Azadirachta indica* root (AIR) carbon is carried out using the impregnation of Fe.

The present study aimed at (i) evaluation of equilibrium adsorption and kinetics using iron impregnated *Azadirachta indica* carbon (new adsorbent) in batch and fixed-bed column operations, (ii) to find the optimum flow velocity, bed height, maximum uptake capacity through the fixed bed column operations to bring the Arsenic concentration in the prescribed domain as per WHO limits. Vast studies carried out where removal of Arsenic is done through different activated carbons using the static batch runs [26]. Very few experiments were conducted in the past using column-based dynamic operations. The novelty of the work is the performance evaluation of *Azadirachta indica* roots derived activated carbon, followed by its impregnation using iron metal. The column experiment which was performed has direct relevance with the large scale industrial operations.

2. Materials and methods

2.1. Apparatus and reagents

Chemicals of analytical grade procured from Merck India limited and used without further purification. Acid washing of glassware followed by rinsing with double distilled water and subjected to oven drying at every stage. Double distilled water was used to prepare reagents. NaOH and HCL having molarity 0.1 were used to maintain the pH.

2.2. Instruments used

Agilent (Laos) inductively coupled mass spectrophotometer (ICPMS)-7900 used to find the concentration of arsenate. The pH of the sample was measured by Hanna (Rhode Island, United States) edge multi parameter pH meter-HI2020. For the study of morphology and Fe-distribution of impregnated iron, Fe-ACs was fractured for exposing internal structure using energy-dispersive X-ray spectroscopy (EDX) coupled with a scanning electron microscope (Carl Zeiss EVO 50, Germany). On the exposed region, no further polishing was done to avoid the spooliation of the surface characteristics of Fe-AIR. Determination of Fe-species was done through X-ray diffraction (XRD) analysis by using Bruker D8 focus (United States) X-ray diffractometer having $\text{Cu-K}\alpha$ X-radiation source and $\lambda = 1.5418$ Å. Brunauer–Emmett–Teller (BET) multipoint technique (Autosorb iQ) was used to evaluate the surface area of impregnated and non-impregnated AIR at 77 K.

2.3. Preparation of arsenic(V) solution

Sodium arsenate ($\text{NaHAsO}_4 \cdot 7\text{H}_2\text{O}$) used to prepare the stock solution of arsenate. Then after, by the dilution of stock solution, required concentrations were obtained. NaOH or H_2SO_4 solution used to control the pH.

2.4. Collection and preparation of adsorbent

The adsorbents which are used in the present work is activated carbon derived from roots of *Azadirachta indica* (Neem) tree, which are further modified by the impregnation procedure with iron salt. The alteration in the structure of pore of activated carbon and enhancement in its surface area is achieved by the impregnation process [27]. More quantity of iron was preferred in the Iron impregnation as the active phase is recognized by the impregnated Iron which is responsible for enhancing adsorption capacity [28].

AIR was purchased from a local timber house. Repeated washing of roots with distilled water was done to remove dust and other impurities, followed by oven drying at 65°C for 30–36 h. After the removal of moisture, the roots were grounded to obtain powder form. The product thus obtained was sieved. The dried mixture was placed in a muffle furnace at 750°C for 6 h. Washing of the product (activated carbon) thus produced was done with distilled water [29]. The washed activated carbon was dried in a hot air oven at 90°C for 6 h. Desiccators are used to store produced activated carbon.

2.4.1. Iron impregnation on the adsorbent

The iron salt solution which is used in the current study for the impregnation, of the activated carbon was obtained by dissolving the ferrous chloride salt in the distilled water. The impregnation method involving thermochemical reactions by ferrous chloride solution was used to coat the activated carbon. The pH of the slurry was maintained at 8 by use of NaOH that enhances the negative charge abundance of activated carbon which in turn enhances the impregnation process [30]. Fifty grams of AC was added to a 500 mL glass beaker filled with a 0.5 M FeCl_2 solution. To prevent precipitation and ferrous oxidation, no headspace was provided. A magnetic stirrer was used for through stirring of AC in the ferrous salt solution. The suspension temperature was controlled and maintained at 70°C . After stirring 24 h, the suspension was collected and filtered by using filter paper. Oven drying at 100°C for 6 h was done to obtain the required solid phase. After complete drying of the solid phase, the product was cooled and washed thoroughly until a clear supernatant was obtained. Post-treatment of the thus obtained product with 1 N NaOH provides the stabilization step in the development of the iron impregnated activated carbon [31].

2.5. Experimental setup

2.5.1. Batch experiments

In the batch experiments, different parameters like time of contact (15–75 min), a dose of adsorbent (0.25–1.25 g), pH (2–10), initial As(V) concentration (50–250 $\mu\text{g/L}$) and

operating temperature (313–328 K) were studied to analyze their effects on As(V) adsorption. In the experimental procedure, a known quantity of Fe-AIR was added to a 250 mL Erlenmeyer flask filled with a 100 mL solution of sodium arsenate ($\text{NaHAsO}_4 \cdot 7\text{H}_2\text{O}$), after pH adjustment. The magnetic stirring of the suspension, thus formed was done till the equilibrium conditions were achieved. After stirring, the suspension was allowed to settle down and filtered using a $0.22 \mu\text{m}$ syringe filter. The obtained filtrate was collected, and the arsenic concentrations were recorded using ICPMS. The following equation [32] was used to calculate adsorption (removal) efficiency:

$$\text{Adsorption (removal) efficiency} = \frac{(C_i - C_e)}{C_i} \times 100 \quad (1)$$

where C_i and C_e are the arsenate concentration before and after treatment in the sample solution.

At equilibrium, the As(V) uptake capacity of Fe-AIR was estimated by the following equation [33]:

$$q_e (\text{uptake capacity}) = \frac{(C_i - C_e)}{M} \times V \quad (2)$$

where M is the mass of the adsorbent and V is the volume of the solution.

The effect of co-existing ions on the adsorption of As(V) was observed at room temperature. The As(V) solution was further spiked with the salts of competing ion, including phosphate (PO_4^{3-}), sulfate (SO_4^{2-}), silicate (SiO_3^{2-}), and nitrate (NO_3^-). At optimum pH and adsorbent dose, the co-existing ion salt solutions were added to 100 ml Erlenmeyer flask, which was already filled with As(V) solution. The suspension thus obtained was subjected to stirring for 10 h. The suspension was filtered through a syringe filter and the resulting concentration was observed as before.

2.5.2. Column experiments

Two experimental setups were constructed for analyzing the adsorptive behavior of As(V) in packed bed reactors. The D.I water spiked with 100 $\mu\text{g/L}$ As(V) at pH of 6 was circulated through the empty column to test the As(V) adsorption in constituents of setup (tubing and column). A little adsorption in the column at the very initial stage was observed, which was vanished off after 3 h, and no adsorption was observed in tubes. Each experimental setup comprise of heat resistant borosilicate glass column (*Reactor 1*: I.D = 2 cm; $H = 30$ cm and *Reactor 2*: I.D = 3 cm; $H = 30$ cm). Both columns were rinsed using 15% nitric acid followed by washing with deionized water at 6 pH for 8 h. Then after, Fe-AIR adsorbent was loaded into the columns. To obtain different bed heights (3, 6, and 9 cm), varying amounts of Fe-AIR (4.17, 10.98, and 17.81 g) were used to pack the column. Layers of glass wool (1 cm) at the ends were used to avoid floating. After loading is done, As(V) spiked water was circulated into the columns by peristaltic pumps with different flow rates (3, 6, and 9 mL/min). The effluents from the column were collected through the weir. Adjustment of optimum pH was done to ensure

the maximum Arsenic uptake for desired concentration and pumped in down-flow mode was used to maintain the desired flow rate. When the concentration of effluent exceeds the value of 99% initial arsenic concentration, the operation was stopped. The hydraulic head of 6 inches was maintained. All samples were collected and refrigerated until their analysis.

Under identical conditions, the blank control test was performed. The amount of As(V) lost during the test was subtracted from the experimental results. All the experiments were performed in triplicate at room 25°C (room temperature). The average experimental values were reported, and the standard deviation was represented using error bars. The relative experimental error was within ±5%.

3. Result and discussion

3.1. Characterization

The scanning electron microscopy (SEM) images (25 kV; 20 μm) of uncarbonized AIR and Fe-AIR at 5000 magnification are shown in Figs. 1 and 2, respectively. SEM images of virgin AIR show smooth and non-porous morphology whereas, SEM image of Fe-AIR reveals the presence of rough, porous, heterogenous, and non-uniform surface. The cavities and heterogeneity of adsorbent support the high adsorption capacity[34]. EDX determined the presence of Fe and Cl, which are known to be good binding agents [35].

The BET surface areas, pore-volume, and pore width of Fe-AIR and virgin AIR are given in Table 2. A reduction in

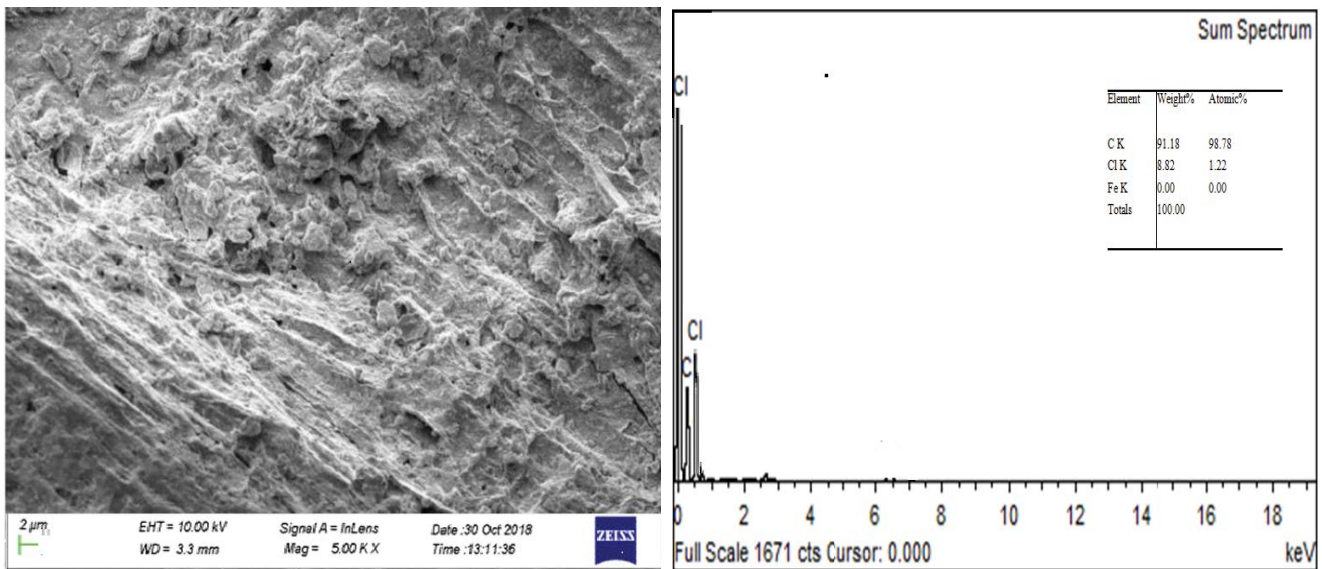


Fig. 1. SEM micrograph and EDX image of AIR.

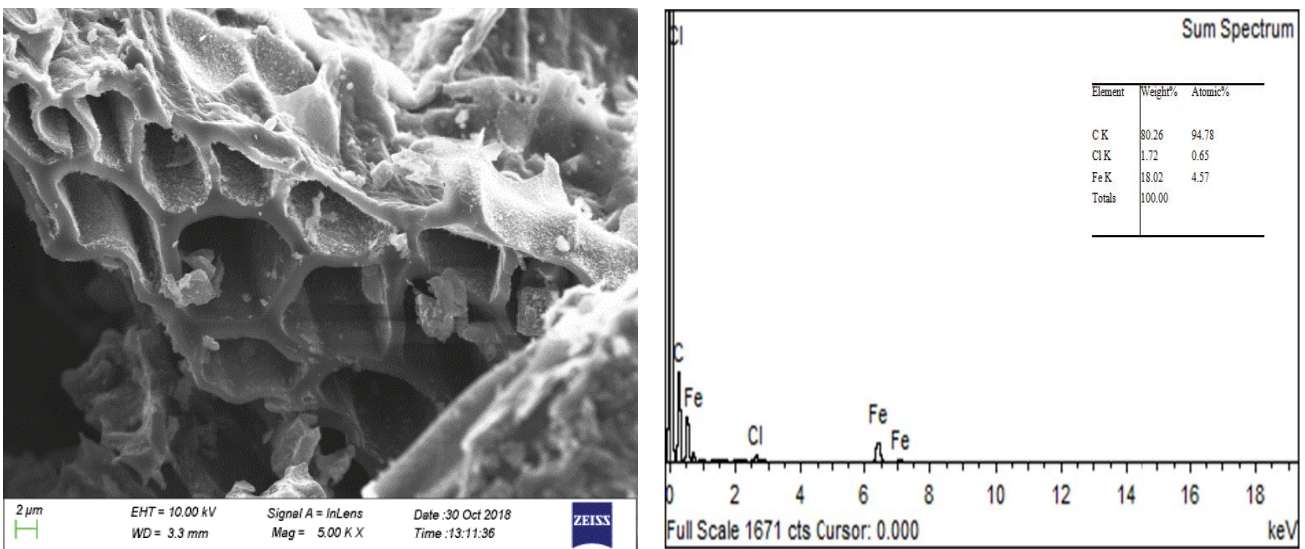


Fig. 2. SEM micrograph and EDX image of Fe-AIR.

Table 1
Physiochemical properties of Fe-AIR

Analysis	Value
Moisture content	11.18%
pH _{zpc}	6.91
pH _{slurry}	6.17
Specific gravity	0.216
Porosity	78%
Particle size	238 μm

Table 2
BET results of virgin AIR and Fe-AIR

	Fe-AC	Virgin AC
Surface area (m^2/g)	358.916	631.355
Pore volume (cc/g)	0.159	0.198
Pore width (\AA)	5.996	23.878

the surface area of Fe-AIR was observed when compared to the surface area of virgin AC. This reduction in surface area can be attributed to the awning of the AIR surface during the impregnation process by iron oxide particles [36]. The pore volume and pore width also decrease in the same fashion as that of BET surface areas from virgin AC to Fe-AC [37]. The pore width of the Fe-AIR lies in the range of 5–15 \AA , which suggests the microporous nature of the adsorbent used in the present study.

Fig. 3 shows the XRD pattern of virgin AIR and Fe-AIR. The XRD plot analysis revealed that the basic structure of AIR carbon is amorphous. Broader peaks were obtained in a 2θ range of 10° – 35° . The peaks of Fe-AIR can be attributed to oxides of iron [38]. The marked peaks of the Fe-AIR plot show the face-centered cubic structure of Fe(II) oxide.

Comparing d values and plot pattern of Fe-AIR with magnetite, it was observed that the peaks of the plots correspond to magnetite which was adsorbed on to the surface of Fe-AIR. No peak corresponds to any other form of Fe was observed. Crystalline nature of adsorbent results from the loading of iron. The absence of a sharp peak in the remaining part of the plot shows porosity and amorphous nature. The appreciable adsorption capacity of Fe-AIR towards arsenic is due to the crystalline, amorphous structure [39].

The electronic state and elemental composition of Fe-AIR in the present study were determined by X-ray photoelectron spectroscopy (XPS) scan. The distribution of the elements on the Fe-AIR was analyzed using the survey scan. Then the concentration of C, O, N, and Fe in the Fe-AIR were measured using utility scans. Fig. 4 shows various positions of peaks of Fe, C, O, and N determined by XPS scan of Fe-AIR. From Fig. 4, it can be seen that the carbon-1s peak was detected at 224.0 eV. The N-1s peak of Fe-AIR was observed at 342.0 eV, which may be due to R-NH₂ (amino) groups in AIR carbon [40]. Strong Fe peaks were observed which can be attributed to effective impregnation of Fe on to AIR. A primary band of Fe at 681.0 eV was observed along with its secondary band at 723.0 eV. The Satellite band of Fe at 698.0 eV can be due to the oxidation state of Fe³⁺ [41]. The presence of Fe³⁺ in Fe-AIR the sample reveals that iron(III) oxide, iron(III) oxide, or residual iron(III) chloride was present on the surface of the sample [42]. No zero-valent Fe was observed on to the Fe-AIR surface in the Fe-2p spectra.

3.2. Batch operations results

3.2.1. Effect of initial arsenate concentration

The influence of initial As(V) concentration on the adsorption of arsenate onto Fe-AIR and AIR, in the concentration range of 50–250 $\mu\text{g}/\text{L}$ is shown in Fig. 5. It can be seen that with increasing concentration of Arsenate, the percentage of removal decreases for both adsorbents. In the

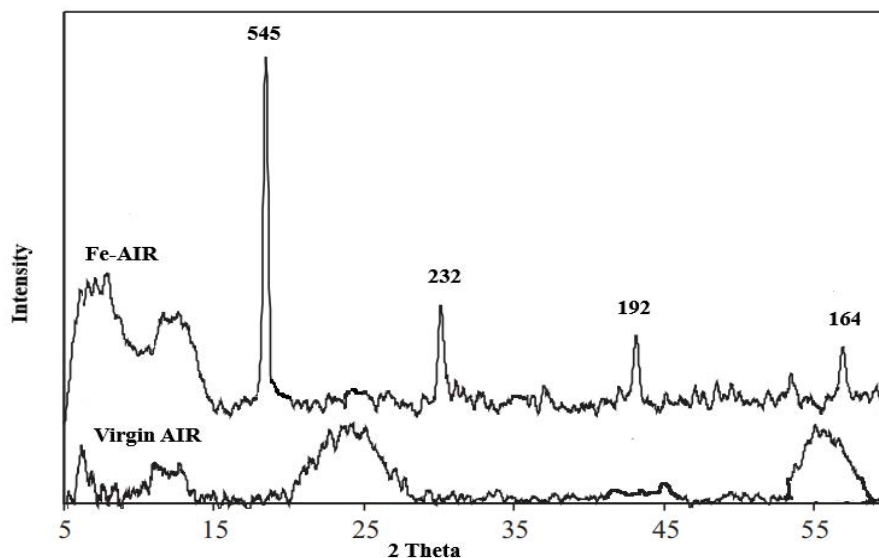


Fig. 3. XRD pattern of Fe-AIR.

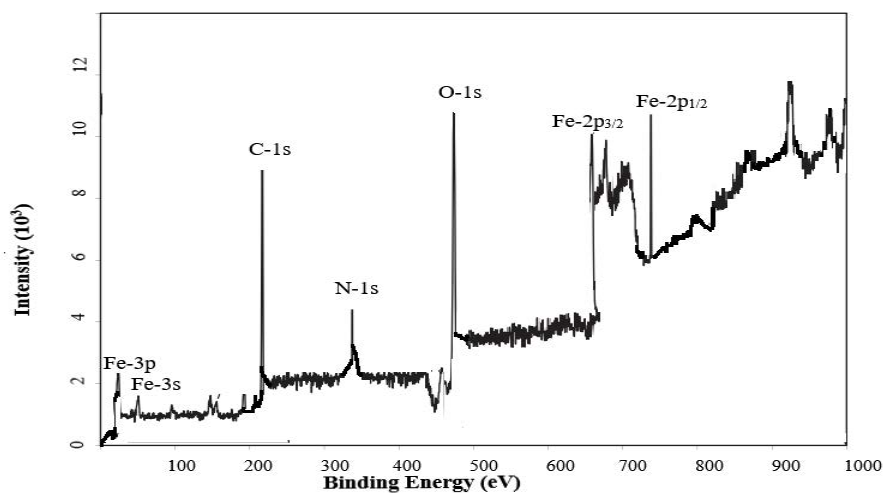


Fig. 4. XPS scans for Fe-AIR.

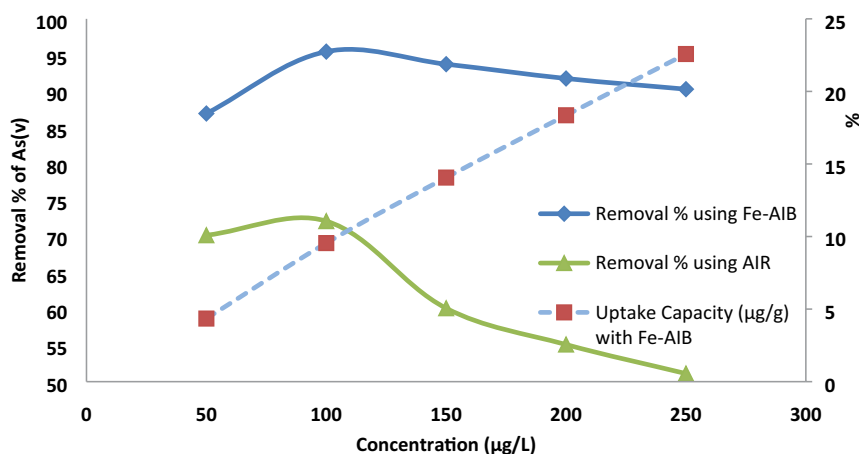


Fig. 5. Effect of initial arsenic concentration on adsorption of arsenate by Fe-AIR.

case of Fe-AIR, removal percentage increases from 90.30% at 250 µg/L to 95.48% at 100 µg/L. Though the adsorption capacity of AIR is comparatively low, the removal percentage increases from 51.11% at 250 µg/L to 72.11% at 100 µg/L, in the same pattern as that in the case of Fe-AIR. The same trend was observed earlier for the adsorption of As(V) with varying initial concentrations [43]. At low As(V) concentration, the adsorption capacity increases due to significant interaction of As(V) ions with the active binding sites and, decrement at high concentration can be attributed to less availability of highly energized binding sites onto the surface of adsorbents [44]. But the amount of Arsenate adsorbed per unit mass of Fe-AIR increases with increasing arsenate concentration in the test solution. This increment can be attributed to reduced solute uptake from solution with an increase in arsenate concentration [45].

3.2.2. Effect of pH on zeta potential and As(V) adsorption

The influence of pH on the As(V) adsorption at AIR and Fe-AIR surface was investigated with an initial As(V)

concentration of 100 µg/L. To each test solution, 1 g of AIR and Fe-AIR was added and equilibrated for 75 min, then after pH and As(V) uptake was recorded. Although adsorption capacity of AIR is very low, maximum As(V) adsorption (73%) onto AIR obtained at pH 4. The adsorption of arsenate is more prominent at acidic conditions. In the pH range of 2–10, anionic behavior is exhibited by As(V) and is replaced by AsO_4^{3-} , HAsO_4^{2-} and H_2AsO_4^- . Under acidic conditions, the surface is positively charged and the accompanying ions balance the positive charge. In this way, ion exchange can take place with anionic species that are already there in a test solution. [46]. It can be seen from Fig. 6 that maximum removal is achieved at pH 5.0–6.0. The isoelectric point (IEP) of Fe-AIR was observed at 6.3, below which Fe-AIR particles are positively charged. The optimum removal of 96.811% (17.7 µg/g) by the Fe-AIR was achieved at a pH of 6.0, which is very close to the IEP point. The following equation will give the surface reaction:



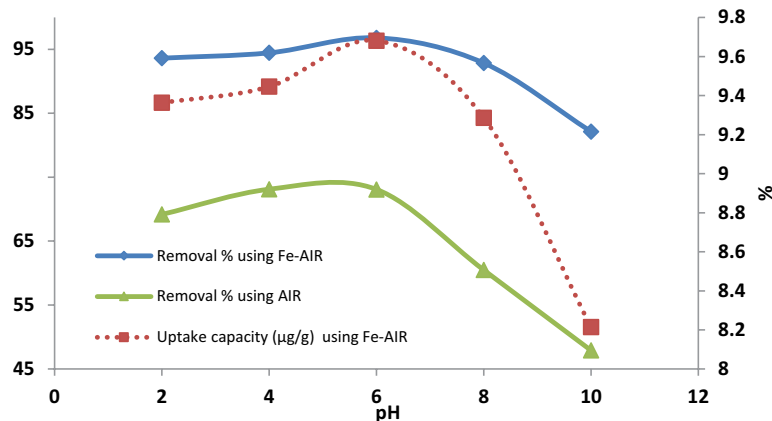
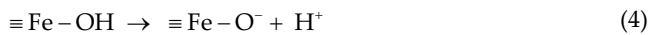


Fig. 6. pH effect on adsorption of As(V) by Fe-AIR.



It can be seen from Fig. 7 that the zeta potential values decrease with increasing pH. This can be attributed to decrement in negative charge on to the surface with increasing pH values. The decrease in negative charge species of As ($\text{H}_2\text{AsO}_4^{2-}$ and HAsO_4^-) is due to the dominance over the adsorption mechanism by electrostatic repulsive forces [47]. After adsorption of As(V) on Fe-AIR, the value of zeta potential decreases. The reason behind this decrement may be the adsorption process resulting from chemisorption and electrostatic attraction (due to inner and outer surface complexation). The final pH of the suspension was lower than the initial pH when the pHs values are greater than 6. This trend can be attributed to the liberation of H^+ ions by Fe-AIR and adsorption of OH^- ions on to the surface at high pHs [48].

There exists one more factor which depends on pH and influences the arsenate adsorption efficiency: pH_{pzc} (point of zero charge) of the adsorbent. The surface charges are more active in acidic conditions which result in a more positive surface charge of Fe-AIR, and hence the attraction towards arsenate is more. The charge on to the surface gets negative when the value of pH exceeds the point of zero charge value due to electrostatic effect (repulsive) and hence the

adsorption capacity of Fe-AIR towards arsenate reduces under basic conditions. The influence of pH on adsorption capacity reported at 5–6 pH values shows the maximum adsorption as these values are less than the point of zero charge (6.9).

3.2.3. Effect of adsorbent dose

The effect of the dose of AIR and Fe-AIR on adsorption of As(V) is illustrated in Fig. 8. The adsorption experiment carried out at an optimum pH of 6 and 100 µg/L initial As(V) concentration. The percentage removal of As(V) was increased from 19.725% to 95.88% as the dose of Fe-AIR increases from 0.25 to 1 g. likewise for AIR removal percentage increases from 23.42% to 67.6% for the same dosages. The increase in adsorption capacities of AIR and Fe-AIR may be due to an increase in surface area, which in turn provides a higher number of active adsorption sites [49]. But above a dose of 1.0 g, the removal of As(V) was negligible for both the adsorbents. This can be attributed to achieving maximum adsorption at a dose of 1.0 g, and hence even with further addition in adsorbent dose, the number of ions will remain unchanged. Similarly, 10 g/L of Fe loaded zeolites shows 98% As(V) removal for 100 µg/L of arsenate concentration [50]. Besides, percent removal

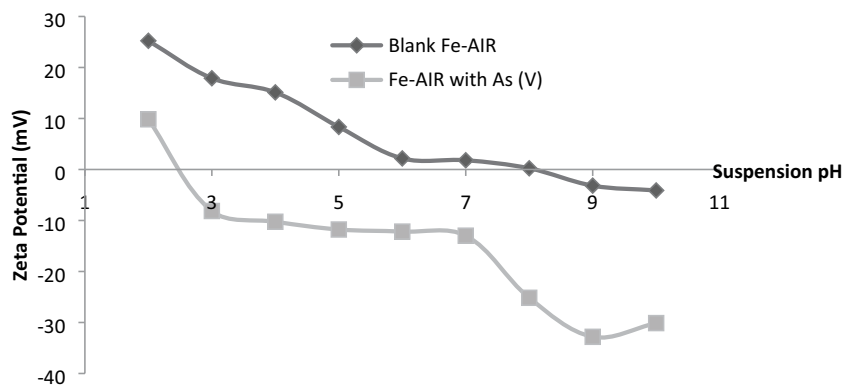


Fig. 7. Zeta-potential of Fe-AIR with and without As(V).

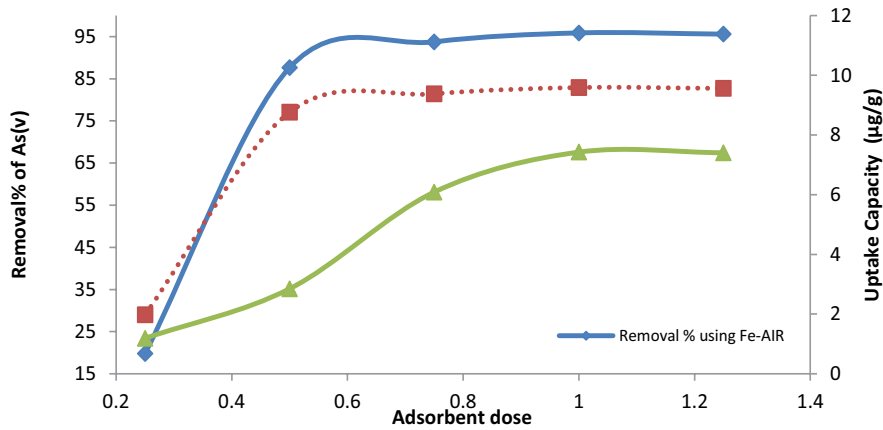


Fig. 8. Effect of dose on arsenate adsorption by Fe-AIR.

of As(V) increases from 20% to 92% using 25–500 mg/L Fe-zeolite [51]. Also, 1 g/L of Fe impregnated bamboo charcoal yields 89% arsenate removal under controlled experimental conditions [52]. More than 97% removal capacity using Fe-biomass carbon (1.5 g/L) was achieved for a test solution containing 10 mg/L of As(V) [53]. Therefore current study shows that a lesser amount of Fe-AIR brings down the As(V) concentration to the prescribed limits. The residual Fe concentrations were also measured after adsorption, and it was observed that at the optimum adsorbent dose the amount of Fe in spent Fe-AIR was 0.152 mg/L. The spent amount was under the maximum permissible limit of Fe (0.2 mg/L) in drinking water by WHO and Fe-AIR can be used as a safe and efficient adsorbent for arsenate removal.

3.2.4. Effect of contact time

The rate of adsorption of As(V) on AIR and Fe-AIR was studied in the time range of 15–75 min Fig. 9 adsorption of As(V) on Fe-AIR is quite rapid, with 94.747% removal of the initial amount within 30 min of operation, and attained equilibrium after approximately 60 min. This behavior is common for As(V) adsorption and has been reported earlier in the literature [40,54]. Larger concentration gradient and

availability of higher adsorption sites attribute to the quick adsorption in the initial stage [54]. After 30 min, no remarkable changes in adsorption capacity were found. Though, the time of contact of 75 min was chosen for maximum removal to take place for the sake of optimization of other process parameters. The adsorption capacity of Fe-AIR was 95.887% at equilibrium ($t = 60$ min).

3.2.5. Influence of the coexisting ions

The results of batch experiments were analyzed by taking As(V) alone as the adsorbate in the test solution. However, in actual practice, several other ions may also be present in contaminated water which can affect the adsorption of As(V) ions. The influence of the presence of other ions including PO_4^{3-} , SO_4^{2-} , SiO_3^{2-} and NO_3^- on the adsorption capacity of Fe-AIR was investigated in a representative test. The percentage removal of As(V) in the absence and presence of competing ions is given in Fig. 10. It was observed that the adsorption capacity of As(V) on Fe-AIR reduced by in the presence of phosphate (PO_4^{3-}) anions. Remarkable reduction in removal percentage was also observed in the presence of SO_4^{2-} anions. The high interference in As(V) adsorption in the presence of phosphates and silicates ions

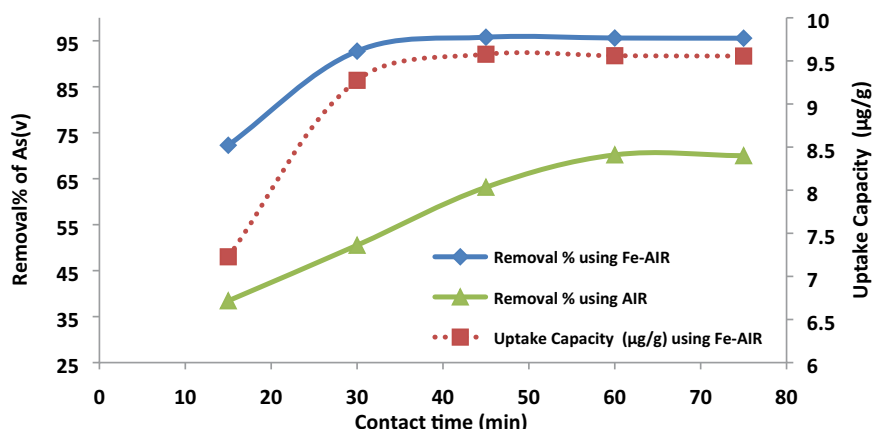


Fig. 9. Effect of contact time on adsorption of arsenate by Fe-AIR.

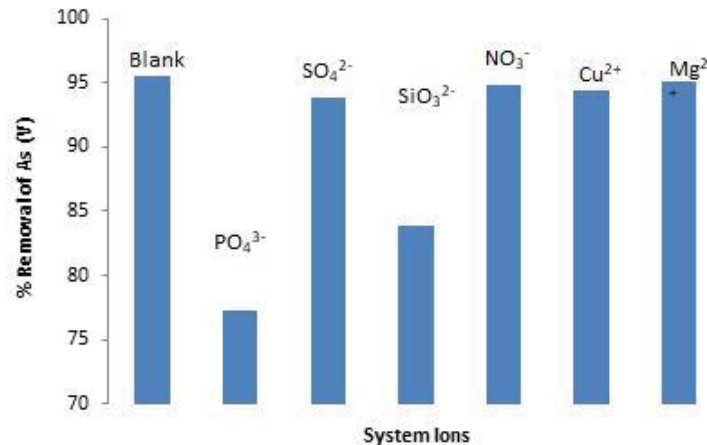


Fig. 10. Effect of co-existing ions on the adsorption of As(V). (Experiment conditions: initial As(V) concentration 100 µg/L; adsorbent dosage 1.0 g/L; solution pH 6.0; agitation speed 60 rpm).

may be attributed to the strong adsorption of these anions onto the Fe oxide surface due to inner core complexation. PO₄³⁻ and SiO₃²⁻ get adsorb by Iron oxide when Complex on the surface is formed with a surface R–OH group [55]. Also, it can be concluded that phosphates and silicates ions possess the same chemical properties as that of arsenate in aqueous solution. Similar results were reported earlier for the removal of As(V) in test solution using the same nature of adsorbents [56,57].

The presence SO₄²⁻ and NO₃⁻ anion does not possess a remarkable impact on the adsorption of As(V) ions. The adsorption of these anions can be due to outer and inner surface complexation. Moreover, their binding ability with oxides of metals is very less when compared to arsenate [58]. The presence of cations does not interfere with the adsorption of As(V).

3.3. Equilibrium adsorption isotherm study for batch process

Isotherm study gives the relationship between the adsorbent and adsorbate. In the current study Langmuir,

Freundlich, Dubinin–Radushkevich (D-R) and, Temkin isotherms equations were used to quantify the removal capacity of Fe-AIR for the adsorption of Arsenate. Langmuir, Freundlich, Temkin models are very significant for chemisorption although the Langmuir and Freundlich isotherm models are equally important for physisorption. Analysis of the physical adsorption of gases and vapors on porous adsorbent is done by D-R isotherm. The assumption of the Langmuir model is based on the fact that adsorbate molecules are bound as a monolayer on to specific sites of the adsorbent surface [59]. Multilayer and heterogeneous adsorption on the adsorbent surface is given by the empirical equation of the Freundlich model. This model takes the assumption that there is an uneven allocation of adsorption sites on the heterogeneous surface [43]. Temkin model gives a corrected adsorption theory involving adsorbate–adsorbent and adsorbate–adsorbate interactions. In the adsorption layer, with an increase in coverage, there is a decrement in the heat of adsorption of all molecules. By taking into account, all the reactions in adsorbate–adsorbent and adsorbate–adsorbate interactions, the adsorption theory was corrected [60]. D-R

Table 3
Isotherm data for sorption of arsenate by Fe-AIR

Adsorption isotherm	Equation	Parameters	Values	R ²
Langmuir isotherm	$\frac{1}{q_e} = \frac{1}{q_{\max} K_L C_e} + \frac{1}{q_{\max}}$	(5) q_{\max} (µg/g) K_L (L/µg)	29.82393 0.102678	0.9918
Freundlich isotherm	$\log q_e = \log K_F + \frac{1}{n} \log C_e$	(6) K_F (µg/g) $1/n$	2.5661 0.5086	0.9899
Temkin isotherm	$q_e = \frac{RT}{b_T} (\ln A_T + \ln C_e)$	(7) A_T (L/µg) b_T (J/mol)	0.720396 324.2599	0.9829
D-R isotherm	$\ln q_e = \ln q_{\max} - \frac{1}{2E^2} \left\{ RT \ln \left(1 + \frac{1}{C_e} \right) \right\}^2$	(8) q_{\max} (µg/g) E (J/mol)	20.05692 7.8991	0.8728

isotherm uses Gaussian energy distribution over a heterogeneous surface to express the mechanism of adsorption. D-R isotherm model is temperature dependent, which is a unique feature on its own [61].

Various correlation coefficients and constants of four adsorption isotherms are evaluated and shown in Table 3. It can be seen from the table, the correlation coefficient for the Langmuir ($R^2 = 0.9918$) model is highest among all four models which shows that the Langmuir model is most relevant to express the equilibrium adsorption of As(V) on Fe-AIR. The removal takes place as monolayer adsorption with homogenous energy levels. Since the separation factor (R_L) value is between 0 and 1, we can say that the adsorption process is favorable. The degree of heterogeneity is given by Freundlich constant (K_F) and another constant n . A graph between $\log(q_e)$ vs. $\log(C_e)$ yields the K_F and $1/n$ values. The value of $1/n$ is coming out to be 0.5086 ($1/n$ value lying between 0 and 1) which shows that adsorption is favorable [62]. Temkin isotherm analysis reveals that the value of heat of adsorption related Temkin constant (B) is 7.6232 which is less than the typical bonding energy range of ion exchange process. The low R^2 value for Temkin isotherm suggests that removal of As(V) by Fe-AIR does not closely follow the isotherm [63]. The E value calculated from the D-R isotherm model equation comes out to be smaller than the typical bonding energy range (8–16 kJ/g) for the process of ion exchange. Thus E value suggests that the adsorption process onto the surface of Fe-AIR may not be only ion exchange mechanism or chemisorption. Thus for adsorption of As(V) by Fe-AIR, pore filling can also be a feasible process [64].

3.4. Kinetic study

The adsorption mechanism, the description of ways of adsorbate molecule transfer and dependency of reaction rate on different variables were studied using kinetics of adsorption. In the present study, to investigate the adsorption mechanism on Fe-AIR at pH 7, 1 g adsorbent at a concentration of 100 $\mu\text{g/L}$ at 298 K temperature, the pseudo-first-order, pseudo-second-order and, intraparticle diffusion models were used. The assumption in the first-order model states that the solute withdrawal rate is proportional to the quantity of adsorbent withdrawal and contrast of concentration at saturation. The rate equation of pseudo-first-order is given by equation [65]:

$$\log\{(q_e) - (q_t)\} = \log\{q_e\} - \frac{k_1}{2.303}t \quad (9)$$

where the quantity of As(V) adsorbed after time t and at equilibrium ($\mu\text{g/g}$) is denoted by q_t and q_e respectively. k_1 is the rate constant for first-order model.

Pseudo-second-order kinetic model assumes that the adsorption process is controlled by chemical adsorption. The rate equation of the second-order model is given by equation [66]:

$$\frac{t}{(q_t)} = \frac{1}{(k_2)(q_e)^2} + \frac{t}{(q_e)} \quad (10)$$

where k_2 is the rate constant for the second-order model. q_t is the arsenate adsorbed after time t and q_e is the arsenate adsorbed on Fe-AIR at equilibrium.

The interphase diffusion plot gives the mechanism of the adsorption process. The Weber–Morris intraparticle model is given by equation [67]:

$$q_t = k_{pi}t^{0.5} + C \quad (11)$$

where q_t is arsenic adsorbed on Fe-AIR after time t , k_{pi} is the intraparticle diffusion rate constant, and constant C gives the thickness of the boundary layer.

Different kinetic model parameters are given in Table 4. The determination coefficient (R^2) will provide the goodness of fit in different models. Higher the value of R^2 , the better will be a description of the kinetics of As(V) adsorption by Fe-AIR. For the entire As(V) concentration range, the first-order model does not give a great fit to experimental data due to the lower determination coefficient. Moreover, adsorption capacity at equilibrium predicted by the first-order model was not in good agreement with the experimental values of q_e . Hence the pseudo-first-order kinetic model was not found suitable for the prediction of the sorption kinetics of As(V) on to Fe-AIR. According to the intraparticle diffusion model, the uptake plot ought to be linear if in the adsorption process, diffusion is twisted and the intraparticle diffusion model is rate-controlling step if the lines originate through the origin. Due to lower R^2 values, the intraparticle diffusion model failed to get fitted

Table 4
Kinetic parameters for adsorption of arsenate by Fe-AIR

Kinetic model	Equation	Parameters	Values	R^2
Pseudo-first-order	$\log\{(q_e) - (q_t)\} = \log\{q_e\} - \frac{k_1}{2.303}t$	q_e k_1	1.7155 0.001317	0.9017
Pseudo-second-order	$\frac{t}{(q_t)} = \frac{1}{(k_2)(q_e)^2} + \frac{t}{(q_e)}$	q_e k_2	10.2832 0.020992	0.9966
Intraparticle diffusion	$q_t = k_{pi}t^{0.5} + C$	k_{pi} C	1.214 5.081	0.8815

with kinetic data and suggests that the rate-controlling step was not intraparticle diffusion for the sorption of Arsenate on to Fe-AIR. Furthermore, the value of the determination coefficient of the pseudo-second-order model was reported as 0.996, which was much higher in comparison to the other models. Also, it was observed that the gap between the experimentally obtained adsorption capacity and the equilibrium adsorption capacity is very narrow for the various concentrations of arsenate which suggest that arsenate on to Fe-AIR follows pseudo-second-order kinetics.

3.5. Thermodynamic studies

Thermodynamics studies provide insight into the nature of the reaction (endothermic or exothermic), entropy, and enthalpy changes resulting from adsorption and change in Gibb's energy. Thermodynamic parameters including change in Gibbs free energy (ΔG°), change in enthalpy (ΔH°), and change in entropy (ΔS°) can be evaluated using equations provided in Table 5 [68]. The negative value of ΔG° reveals that the adsorption is feasible and spontaneous, maybe resulting from columbic attraction. Also, decrement in ΔG° values with increment in temperature propound that adsorption of As(V) on Fe-AIR is even more favorable at elevated temperatures. The positive value of ΔH° (5.33092×10^{-3}) reveals that the adsorption of As(V) on Fe-AIR is an endothermic process [69]. The degree of randomness of the system has been defined as entropy. A positive value of entropy change confers the structural changes that occurred on the surface of adsorbent during the adsorption process and randomness increases in the adsorption system at solid-liquid interphase [70].

3.6. Column operations results

3.6.1. Effect of bed height

The bed depth of the adsorbent in the column is a key parameter for adsorption as segregation of metal ions is dependent on the amount of adsorbent inside the column. The influence of bed depth on breakthrough was analyzed by carrying out adsorption experiments in bed height ranging from 3–9 cm, at optimum pH, constant influent Arsenate concentration (1,000 $\mu\text{g/L}$) and, flow rate (3.0 mL/min). Breakthrough curves for adsorption of As(V) on Fe-AIR are shown in Fig. 11. The effect of bed height can be evaluated from the shape of the breakthrough and time needed

to attain a breakthrough point. Larger bed heights result in the availability of more time for interaction of Fe-AIR with As(V), which in turn enhances the diffusion of As(V) ions into the Fe-AIR and adsorption capacity of Fe-AIR increases with increasing bed height [71]. Similar results showing the increment in exhaustion time with increasing bed height were reported earlier in literature [72,73].

3.6.2. Effect of flow rate

The flow rate is an important parameter that affects the adsorption process in a continuous flow column to a great extent. In the current study, the influence of flow rate on Arsenate adsorption by Fe-AIR was investigated by varying the flow rate from 3.0 to 9.0 mL/min and keeping the influent arsenate concentration (1,000 $\mu\text{g/L}$), bed height (9.0 cm) and pH constant. The breakthrough curve is shown in Fig. 12. It was observed that for higher flow rates, a quicker breakthrough was achieved. With decreasing flow rates, a significant increase in breakthrough time was noted. At a low inlet flow rate of As(V), time available for interaction with Fe-AIR was more which in turn results in increased removal of As(V) ions in the column. Fundamental of mass transfer demonstrates the variation in adsorption capacity and slope of the breakthrough curve. The explanation is that increased flow rate results in enhanced mass transfer rate and the amount of As(V) adsorbed onto mass transfer zone (unit bed height) increases, due to which faster saturation was achieved [74]. Less residence time of As(V) ions in column resulted in reduced adsorption capacities at an increased flow rate and solutes leave the column before the occurrence of equilibrium. These findings were in good agreement with results referred to the previous literature [75,76].

3.6.3. Effect of influent As(V) concentration

The influence of varying As(V) concentration ranging from 1,000–1,500 $\mu\text{g/L}$ with 9 cm of Fe-AIR bed height and influent As(V) flow rate of 3 mL/min is shown by the breakthrough curve in Fig. 13. As can be seen from fig, in the time interval of 400 min, the C_t/C_i values reach 0.50, 0.67 and 0.89 when influent concentration was 1,000; 1,250; and 1,500 $\mu\text{g/L}$ respectively. It is observed that with increasing influent As(V) concentration, the breakthrough time decreases. A slower and dispersed breakthrough

Table 5
Thermodynamic parameters for adsorption of arsenate by Fe-AIR

Thermodynamics parameters	Equation	Values	
		Temp. (K)	ΔG° (KJ/mol)
Standard Gibbs free energy	$\Delta G^\circ = -RT \ln K_c$	313	-1.79076
		318	-1.82576
		323	-1.85492
		328	-1.88409
Standard enthalpy change	$\log K_c = \frac{\Delta S^\circ}{2.303R} - \frac{\Delta H^\circ}{2.303RT}$	$\Delta H^\circ = 1.58007$	
Standard entropy change		$\Delta S^\circ = 5.33092 \times 10^{-3}$	

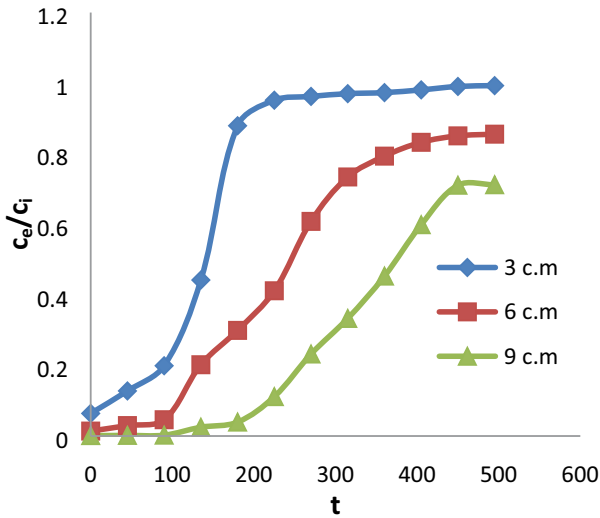


Fig. 11. The breakthrough curve for arsenate adsorption by Fe-AIR at different bed height.

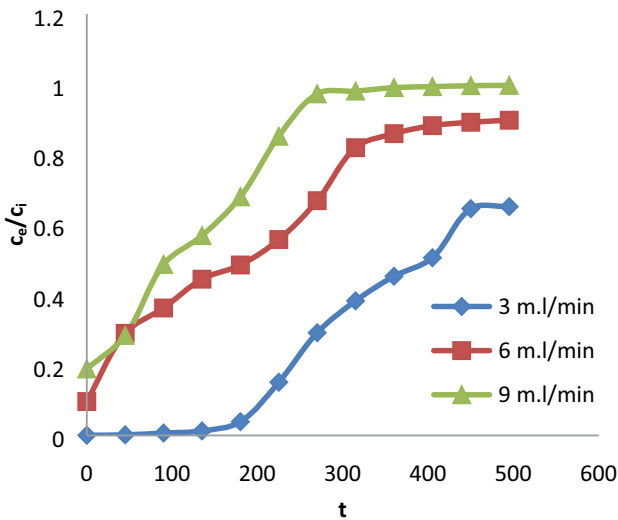


Fig. 12. The breakthrough curve for arsenate adsorption by Fe-AIR at different flow rates.

was analysed at lower concentration and sharper breakthrough curves were obtained at higher concentration. This can be attributed to slow transport of As(V) ions resulted from a decreased diffusion coefficient. The slope of the curve became steeper with increasing influent concentration. These findings show that the rate of saturation and breakthrough time was influenced by the variation of concentration gradient which means the process of diffusion is dependent on concentration. The loading rate of As(V) ions increases with increasing influent concentration along with the increase in driving force and the length of the adsorption zone decreases [77]. Similar behaviour was observed for As(V) removal by Fe-oxide based adsorbent [78], Arsenate adsorption on untreated dolomite powder [79]. With increasing influent concentration, the increase in adsorption capacity was expected due to enhanced driving

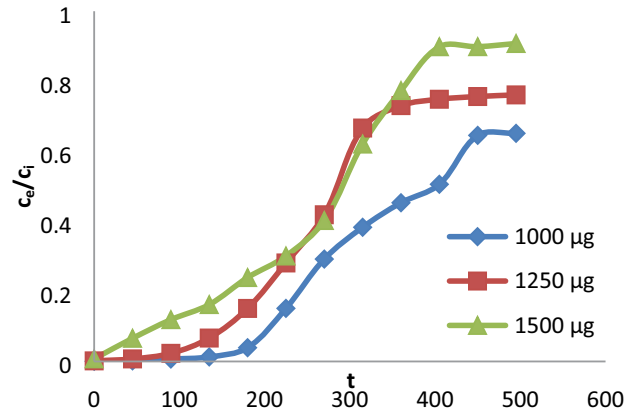


Fig. 13. The breakthrough curve for arsenate adsorption by Fe-AIR at different influent concentration.

force facilitated by a higher concentration difference for the adsorption process. The largest bed capacity of 90.02 µg/g was achieved using 1,000 µg/L influent As(V) concentration, 9 cm bed height, and 3 mL/min flow rate. The present result is in agreement with fixed bed adsorption operations which were reported earlier [80,81].

3.6.4. Effect of the column diameter

The effect of the column diameter (2 and 3 cm) at a fixed bed height of 9 cm, a flow rate of 3.0 mL/min, and normal pH is shown in Fig. 14. It was observed that maximum removal of 92.785% was achieved using a 3 cm diameter column having the same height and influent metal concentration like that of a 2 cm diameter column. This can be attributed to the fact that larger depth is achieved in the column having a larger diameter which in turn increases the interaction between the As(V) solution and the adsorbent permitting better adsorption of As(V) ion at available binding sites of Fe-AIR [82].

3.6.5. Thomas model application

One of the most extensively used and general models for packed column studies is the Thomas model. The assumptions used in the Thomas model are that axial dispersion is not there and it follows Langmuir adsorption kinetics, provided that the second-order kinetics is obeyed by rate deriving force. A constant separation factor is also assumed but applies to unfavorable or favorable isotherm. Thomas model also possesses some disadvantages like its derivation is based on second-order kinetics. Interphase mass transfer often controls adsorption and is not limited by chemical kinetics. Some errors may results from all these discrepancies while the adsorption process is being modeled using the Thomas model [83]. The model has the following linearized form:

$$\frac{C_t}{C_0} = \frac{1}{1 + \exp\left(K_{TH}q_0 \frac{m}{Q} - K_{TH}C_0t\right)} \quad (14)$$

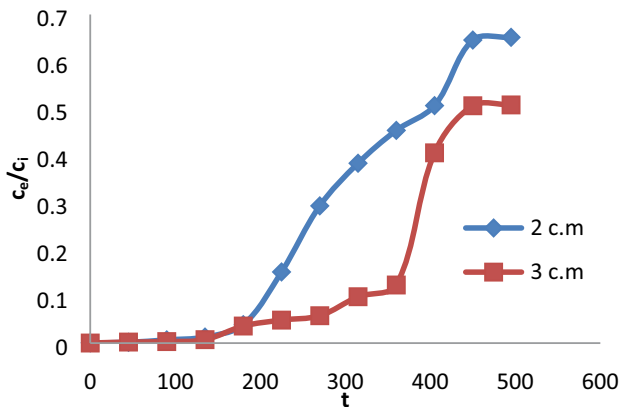


Fig. 14. The breakthrough curve for arsenic adsorption by Fe-AIR at different column diameters.

where C_0 and C_t are As(V) concentrations initially and after time t respectively, q_0 is As(V) uptake per gram ($\mu\text{g/g}$) of Fe-AIR at equilibrium, m is the mass of As(V) in grams, the flow rate is given by Q (mL/min) and K_{TH} is Thomas constant (L/ $\mu\text{g min}$). Table 6 shows the values of Thomas constants and As(V) uptake capacity at different bed heights, flow rates, influent arsenic concentration, and column diameters. It can be seen from the table that all the mentioned parameters affect Thomas constant and As(V) uptake capacity. The values of As(V) uptake capacity increase and Thomas constant (K_{TH}) reduces with increasing bed height. With increasing flow rates, the values of As(V) uptake capacity decreases and Thomas constant (K_{TH}) increases. Also, with increasing influent arsenic concentration, K_{TH} decreases and As(V) uptake capacity increases. Also with an increase in column diameter, both K_{TH} and q_0 values increases. The same trend has been reported earlier [84].

3.6.6. Yoon–Nelson model application

Yoon–Nelson model does not concentrate on the nature of adsorbent, adsorbate properties, and any physical aspects of adsorption bed and it's a straightforward physical assumption. Yoon–Nelson model states that adsorption rate decrement is proportional to adsorption of adsorbate and adsorbent breakthrough [85]. The following expression is used:

$$\ln \frac{C_t}{C_0} = K_{\text{YN}} t - K_{\text{YN}} \tau \quad (15)$$

where K_{YN} is velocity constant and τ is the time needed for fifty percent adsorbate breakthrough. The values of τ and K_{YN} can be obtained from the intercept and slope of the linear graph of $\ln C_t/C_0$ and t . The table shows values of T and K_{YN} at various bed heights, flow rates, influent arsenic concentration, and column diameters. It can be concluded from Table 6 that with increasing influent arsenic concentration, the K_{YN} values increase. This may be attributed to the fact that with increment in initial concentration, vying for the binding sites among adsorbate molecules increases which results in enhanced uptake capacity of Fe-AIR. The values of K_{YN} increases with an increase in bed height and decrease with an increase in column diameter.

3.6.7. Regeneration and reuse of Fe-AIR

For a feasible adsorption process, it is important to have efficient regeneration and reuse of adsorption medium. To test the same, the 9 cm exhausted Fe-AIR media was regenerated using NaOH (10%). The recovery profile of arsenate through desorption is shown in Fig. 15. It can be concluded from the calculations that for 99% arsenate recovery, 12-bed volumes are sufficient. Almost 83.5% of adsorbed arsenate was eluted during the first two bed volumes and

Table 6
Column operation modeling results onto Fe-AIR column

Process parameters		Thomas model results			Yoon–Nelson model results	
Bed height (cm)	q_{exp} ($\mu\text{g/g}$)	K_{TH} (mL/min μg)	q_0 ($\mu\text{g/g}$)	R^2	K_{YN}	τ
3	70.75	0.017	64.21	0.83	0.010	135.30
6	85.33	0.012	76.52	0.95	0.015	287.17
9	89.15	0.010	90.89	0.93	0.016	388.03
Flow rate (mL/min)						
3	89.1541	0.0067	90.8981	0.9339	0.0168	388.0347
6	84.0307	0.0084	81.2042	0.9468	0.0084	187.3247
9	76.2183	0.0104	63.2949	0.9521	0.0157	97.3405
Conc. in ($\mu\text{g/L}$)						
1,000	89.1541	0.0104	90.0222	0.9339	0.0133	388.0347
1,250	90.2231	0.0095	90.8981	0.9245	0.0153	332.2661
1,500	92.6643	0.0088	91.0536	0.9548	0.0168	280.0608
Column dia. (cm)						
2	89.1541	0.01045	90.8981	0.9339	0.0168	388.0347
3	93.3372	0.01605	97.4687	0.7455	0.0160	449.6885

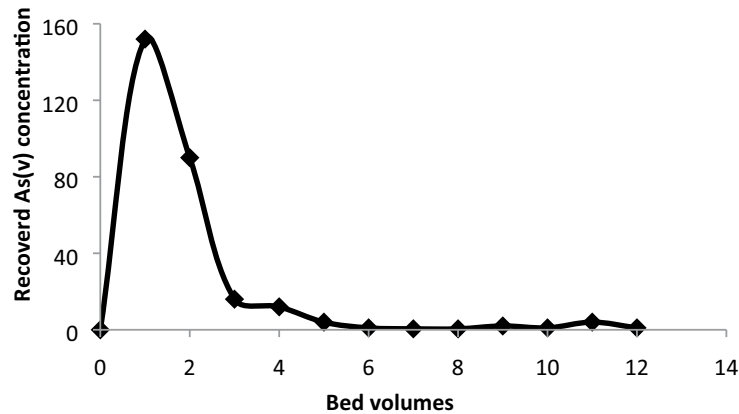


Fig. 15. Concentration profile of arsenate during regeneration.

the rest get removed in the next 10 bed volumes. From these findings, it can be concluded that the active sites of Fe-AIR particles are accessible through the pore network among the particles, which suggests that there occurs no clogging in pores.

After regeneration, excess NaOH was removed through the conditioning process where media was subjected to hot water, due to which the pH was decreased. The concentration of dissolved iron in the regenerant spent was reported as 0.02 mg/L, which is very low in comparison to the amount of iron present in the medium. So it was assumed that the total amount of Fe in the medium remains unaltered. Fig. 16 shows six adsorption cycles. It can be seen from the figure that appreciable decrement of 31.4% in the removal percentage was observed after 5 cycles. Hence it can be concluded from regeneration and reuse analysis that Fe-AIR proffers an inexpensive approach to the removal of arsenate from water.

3.6.8. Adsorption capacity comparison of different adsorbents from the literature for removal of As(V)

The adsorption potential of Fe-AIR needs to be compared with other adsorbents used for the purpose to justify

its validity. The value of q_{\max} at different operating conditions is listed in Table 7. It is not possible to compare the adsorption capacity of Fe-AIB and Fe-AIL directly with other adsorbents due to different operating conditions. However, the adsorbent used in the present study shows good adsorption capacity when compared with other adsorbents. The variation in adsorption capacity for different adsorbents are due to difference in individual properties (functional group, surface structure, available surface area) of adsorbents

4. Conclusion

A methodology of Fe impregnation was applied to synthesize a porous cost-effective arsenate adsorbent (Fe-AIR) from the *Azadirachta indica* roots carbon. The adsorption capacity and efficiency of Fe-AIR for remediation of arsenate from contaminated waters were investigated. Batch operations were conducted under various operating conditions to analyze the adsorption capacity of Fe-AIR. The maximum removal of arsenate species on Fe-AIR from arsenate spiked deionized water is reported to be 96.811%. Analysis of the effect of competing ions reveals that the presence of phosphate and sulfate anions reduces the adsorption capacity whereas the presence of cations does not affect the

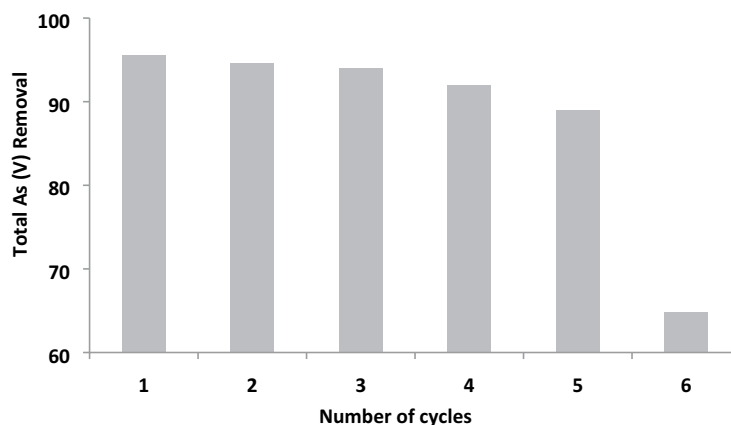


Fig. 16. Variation in percentage removal of As(V) by repetitive use of Fe-AIR.

Table 7

Comparison of adsorption capacity of various adsorbent adsorbents used for As(V) remediation

Adsorbent	Conditions	q_{\max} (mg/g)	Reference
Green marine algal-based biochar	pH 4.0; flow rate 5 mL/min; dose 12.66 g	7.67	[86]
Lamdong laterite soil	pH 3.0; flow rate 11.2 mL/min; bed depth 2.7 cm	0.47	[87]
Activated alumina impregnated by Fe oxide	pH 12.0; flow rate 16 mL/min; bed depth 6 cm	0.46	[88]
Biopolymer chitosan sorbent	pH 7.0; flow rate 8 mL/min; bed depth 8 cm	1.90	[89]
Fe-oxide coated cement	pH 6.0; flow rate 1.35 mL/min; bed depth 10 cm; influent concentration 2.7 mg/L	2.3	[90]
Waste of rice husk	pH 5.0–6.0; flow rate 6.7 mL/min; bed depth 5 cm; influent concentration 0.1 mg/L	0.007	[32]
Iron-zein beads	pH 6.0; flow rate 4 mL/min; bed depth 3 cm; influent concentration 0.5–100 mg/L	1.95	[91]
Composite of Fe oxides and carbon with eucalyptus wood	pH 3.0; flow rate 5.136 mL/min; dose 2 g; influent concentration 20 mg/L	10.49	[92]
Poly LDHs	pH 8.0; flow rate 7 mL/min; initial concentration 50 mg/L	1.73	[93]
Iron impregnated <i>Azadirachta indica</i> roots carbon (Fe-AIR)	pH 6.0; flow rate 3.0 mL/min; bed depth 3 cm; influent concentration 1 mg/L	0.093	Present study

adsorption process. The batch process was evaluated by various isotherms and kinetic models. Langmuir isotherm best fits the batch operation data. From the results of adsorption kinetics, it can be seen that the second-order kinetics controls the adsorption. The exothermic nature of adsorption was observed. Spontaneous adsorption on Fe-AIR was indicated from negative values of ΔG° . To analyze the practical applicability of Fe-AIR in the removal of Arsenate species, column operations were employed. The experimental data of column operations fits well with Thomas model and Yoon–Nelson model for arsenic influent concentration ranging from 1,000–1,500 ppb at a flow rate of 3 mL/min. Following adsorption, about 99% of Fe-AIR fixed bed was regenerated effectively with 10% sodium hydroxide within 12-bed volumes. Not much depression in efficiency is reported in the first five cycles, which makes Fe-AIR responsive to reuse and regeneration and thus cost-effective in use. Through arsenic incorporation in Portland cement, arsenic solidification is possible so there will not be an issue of secondary pollution. Moreover, the developed fixed column treatment process is easy to handle, reproducible, rapid, and economic so it is a suitable and appropriate approach for arsenic remediation in local areas.

Acknowledgment

The authors would like to thank Post Graduation Research Lab, IIT Kanpur for providing assistance with SEM, XRD, BET, and FTIR analysis.

References

- [1] M. Kobya, R.D.C. Soltani, P.I. Omwene, A. Khataee, A review on decontamination of arsenic-contaminated water by electrocoagulation: reactor configurations and operating cost along with removal mechanisms, *Environ. Technol. Innovation*, 17 (2020) 100519.
- [2] S. Alka, S. Shahir, N. Ibrahim, T.-T. Chai, Z. Mohd Bahari, F. Abd Manan, The role of plant growth promoting bacteria on arsenic removal: a review of existing perspectives, *Environ. Technol. Innovation*, 17 (2020) 100602.
- [3] P. Kumarathilaka, S. Seneweera, Y.S. Ok, A.A. Meharg, J. Bundschuh, Mitigation of arsenic accumulation in rice: an agronomical, physico-chemical, and biological approach – a critical review, *Crit. Rev. Environ. Sci.*, 50 (2020) 31–71.
- [4] S.K. Gupta, K.Y. Chen, Arsenic removal by adsorption, *Water Pollut. Control Fed.*, 50 (1978) 493–506.
- [5] A. Maiti, S. DasGupta, J.K. Basu, S. De, Batch and column study: adsorption of arsenate using untreated laterite as adsorbent, *Ind. Eng. Chem. Res.*, 47 (2008) 1620–1629.
- [6] F. Fu, Q. Wang, Removal of heavy metal ions from wastewaters: a review, *J. Environ. Manage.*, 92 (2011) 407–418.
- [7] M.E. Argun, S. Dursun, C. Ozdemir, M. Karatas, Heavy metal adsorption by modified oak sawdust: thermodynamics and kinetics, *J. Hazard. Mater.*, 141 (2007) 77–85.
- [8] A. Demirbas, Heavy metal adsorption onto agro-based waste materials: a review, *J. Hazard. Mater.*, 157 (2008) 220–229.
- [9] D. Sud, G. Mahajan, M.P. Kaur, Agricultural waste material as potential adsorbent for sequestering heavy metal ions from aqueous solutions—a review, *Bioresour. Technol.*, 99 (2008) 6017–6027.
- [10] S.E. Bailey, T.J. Olin, R.M. Bricka, D.D. Adrian, A review of potentially low-cost sorbents for heavy metals, *Water Res.*, 33 (1999) 2469–2479.
- [11] D. Gnanasangeetha, D. SaralaThambavani, Modelling of As³⁺ adsorption from aqueous solution using *Azadirachta indica* by artificial neural network, *Desal. Water Treat.*, 56 (2015) 1839–1854.
- [12] T.R. Choudhury, M. Amin, S. Quraishi, A. Mustafa, Arsenic(III) removal from real-life groundwater by adsorption on Neem Bark (*Azadirachta indica*), *Int. Res. J. Pure Appl. Chem.*, (2014) 594–604.
- [13] P. Roy, U. Dey, S. Chattoraj, D. Mukhopadhyay, N.K. Mondal, Modeling of the adsorptive removal of arsenic(III) using plant biomass: a bioremediation approach, *Appl. Water Sci.*, 7 (2017) 1307–1321.
- [14] A. Bhattacharya, S. Mandal, S. Das, Adsorption of Zn(II) from aqueous solution by using different adsorbents, *Chem. Eng. J.*, 123 (2006) 43–51.
- [15] D. Tiwari, S.P. Mishra, M. Mishra, R. Dubey, Biosorptive behavior of Mango (*Mangifera indica*) and Neem (*Azadirachta*

- indica*) bark for Hg²⁺, Cr³⁺, and Cd²⁺ toxic ions from aqueous solutions: a radiotracer study, *Appl. Radiat. Isot.*, 50 (1999) 631–642.
- [16] A. Bhattacharya, T. Naiya, S. Mandal, S. Das, Adsorption, kinetics and equilibrium studies on removal of Cr(VI) from aqueous solutions using different low-cost adsorbents, *Chem. Eng. J.*, 137 (2008) 529–541.
- [17] R. Srivastava, D.C. Rupainwar, A comparative evaluation for adsorption of dye on Neem bark and Mango bark powder, *Indian J. Chem. Technol.*, 18 (2011) 67–75.
- [18] S.W. Al Rmalli, C.F. Harrington, M. Ayub, P.I. Haris, A biomaterial based approach for arsenic removal from water, *J. Environ. Monit.*, 7 (2005) 279–282.
- [19] S. Zhu, J. Zhao, N. Zhao, X. Yang, C. Chen, J. Shang, Goethite modified biochar as a multifunctional amendment for cationic Cd(II), anionic As(III), roxarsone, and phosphorus in soil and water, *J. Cleaner Prod.*, 247 (2020) 119579.
- [20] H. Lyu, J. Tang, M. Cui, B. Gao, B. Shen, Biochar/iron (BC/Fe) composites for soil and groundwater remediation: synthesis, applications, and mechanisms, *Chemosphere*, 246 (2020) 125609.
- [21] S. Ali, M. Rizwan, M.B. Shakoor, A. Jilani, R. Anjum, High sorption efficiency for As(III) and As(V) from aqueous solutions using novel almond shell biochar, *Chemosphere*, 243 (2020) 125330.
- [22] T. Chen, X. Quan, Z. Ji, X. Li, Y. Pei, Synthesis and characterization of a novel magnetic calcium-rich nanocomposite and its remediation behavior for As(III) and Pb(II) co-contamination in aqueous systems, *Sci. Total Environ.*, 706 (2020) 135122.
- [23] J. Cui, Q. Jin, Y. Li, F. Li, Oxidation and removal of As(III) from soil using novel magnetic nanocomposite derived from biomass waste, *Environ. Sci. Nano*, 6 (2019) 478–488.
- [24] L. Verma, M.A. Siddique, J. Singh, R.N. Bharagava, As(III) and As(V) removal by using iron impregnated biosorbents derived from waste biomass of *Citrus limmeta* (peel and pulp) from the aqueous solution and ground water, *J. Environ. Manage.*, 250 (2019) 109452.
- [25] H. Zeng, Y. Yu, F. Wang, J. Zhang, D. Li, Arsenic(V) removal by granular adsorbents made from water treatment residuals materials and chitosan, *Colloids Surf., A*, 585 (2020) 124036.
- [26] M.K. Mondal, R. Garg, A comprehensive review on removal of arsenic using activated carbon prepared from easily available waste materials, *Environ. Sci. Pollut. Res.*, 24 (2017) 13295–13306.
- [27] I. Shah, R. Adnan, W.S. Wan Ngah, N. Mohamed, Iron impregnated activated carbon as an efficient adsorbent for the removal of Methylene blue: regeneration and kinetics studies, *PLoS One*, 10 (2015) e0122603.
- [28] Y. Sudaryanto, T. Deitiana, W. Irawaty, H. Hindarso, S. Ismadji, High surface area activated carbon prepared from cassava peel by chemical activation, *Bioresour. Technol.*, 97 (2006) 734–739.
- [29] S. Rahdar, M. Taghavi, R. Khaksefidi, S. Ahmadi, Adsorption of arsenic(V) from aqueous solution using modified saxaul ash: isotherm and thermodynamic study, *Appl. Water Sci.*, 9 (2019) 87.
- [30] Gh. Ghanizadeh, M.H. Ehrampoush, M.T. Ghaneian, Application of iron impregnated activated carbon for removal of arsenic from water, Iran. *J. Environ. Health Sci. Eng.*, (ISSN: p-ISSN: 1735–1979), 7 (2010) 145–156.
- [31] Q. Chang, W. Lin, W.-c. Ying, Preparation of iron-impregnated granular activated carbon for arsenic removal from drinking water, *J. Hazard. Mater.*, 184 (2010) 515–522.
- [32] M.N. Amin, S. Kaneco, T. Kitagawa, A. Begum, H. Katsumata, T. Suzuki, K. Ohta, Removal of arsenic in aqueous solutions by adsorption onto waste rice husk, *Ind. Eng. Chem. Res.*, 45 (2006) 8105–8110.
- [33] B.M. Lekić, D.D. Marković, V.N. Rajaković-Ognjanović, A.R. Dukić, L.V. Rajaković, Arsenic removal from water using industrial by-products, *J. Chem.*, 2013 (2013) 9.
- [34] M.A. Alam, W.A. Shaikh, M.O. Alam, T. Bhattacharya, S. Chakraborty, B. Show, I. Saha, Adsorption of As(III) and As(V) from aqueous solution by modified *Cassia fistula* (golden shower) biochar, *Appl. Water Sci.*, 8 (2018) 198.
- [35] M.L. Paul, J. Samuel, N. Chandrasekaran, A. Mukherjee, Comparative kinetics, equilibrium, thermodynamic and mechanistic studies on biosorption of hexavalent chromium by live and heat killed biomass of *Acinetobacter junii* VITSUKMW2, an indigenous chromite mine isolate, *Chem. Eng. J.*, 187 (2012) 104–113.
- [36] S. Nethaji, A. Sivasamy, A.B. Mandal, Preparation and characterization of corn cob activated carbon coated with nano-sized magnetite particles for the removal of Cr(VI), *Bioresour. Technol.*, 134 (2013) 94–100.
- [37] M. Dinesh, S. Ankur, V.K. Singh, M. Alexandre-Franco, C.U. Pittman Jr., Development of magnetic activated carbon from almond shells for trinitrophenol removal from water, *Chem. Eng. J.*, 172 (2011) 1111–1125.
- [38] T. Depci, Comparison of activated carbon and iron impregnated activated carbon derived from Gölbaşı lignite to remove cyanide from water, *Chem. Eng. J.*, 181 (2012) 467–478.
- [39] L.G. Sorokhaibam, V.M. Bhandari, M.S. Salvi, S. Jain, S.D. Hadawale, V.V. Ranade, Development of newer adsorbents: activated carbons derived from carbonized *Cassia fistula*, *Ind. Eng. Chem. Res.*, 54 (2015) 11844–11857.
- [40] D.D. Gang, B. Deng, L. Lin, As(III) removal using an iron-impregnated chitosan sorbent, *J. Hazard. Mater.*, 182 (2010) 156–161.
- [41] B. Sunkara, J. Zhan, I. Kolesnichenko, Y. Wang, J. He, J.E. Holland, G.L. McPherson, V.T. John, Modifying metal nanoparticle placement on carbon supports using an aerosol-based process, with application to the environmental remediation of chlorinated hydrocarbons, *Langmuir*, 27 (2011) 7854–7859.
- [42] M. Descostes, F. Mercier, N. Thromat, C. Beaucaire, M. Gautier-Soyer, Use of XPS in the determination of chemical environment and oxidation state of iron and sulfur samples: constitution of a data basis in binding energies for Fe and S reference compounds and applications to the evidence of surface species of an oxidized pyrite in a carbonate medium, *Appl. Water Sci.*, 165 (2000) 288–302.
- [43] M.B. Baskan, A. Pala, Batch and fixed-bed column studies of arsenic adsorption on the natural and modified clinoptilolite, *Water Air Soil Pollut.*, 225 (2014) 1798.
- [44] P. Chutia, S. Kato, T. Kojima, S. Satokawa, Arsenic adsorption from aqueous solution on synthetic zeolites, *J. Hazard. Mater.*, 162 (2009) 440–447.
- [45] H. Nollet, M. Roels, P. Lutgen, P. Van der Meer, W. Verstraete, Removal of PCBs from wastewater using fly ash, *Chemosphere*, 53 (2003) 655–665.
- [46] R. Ansari, M. Sadegh, Application of activated carbon for removal of arsenic ions from aqueous solutions, *E-J. Chem.*, 4 (2007) 103–108.
- [47] L.H. Velazquez-Jimenez, J.A. Arcibar-Orozco, J.R. Rangel-Mendez, Overview of As(V) adsorption on Zr-functionalized activated carbon for aqueous streams remediation, *J. Environ. Manage.*, 212 (2018) 121–130.
- [48] N.D.G. Chau, Z. Sebesvari, W. Amelung, F.G. Renaud, Pesticide pollution of multiple drinking water sources in the Mekong Delta, Vietnam: evidence from two provinces, *Environ. Sci. Pollut. Res.*, 22 (2015) 9042–9058.
- [49] Y. Li, F.S. Zhang, F.R. Xiu, Arsenic(V) removal from aqueous system using adsorbent developed from a high iron-containing fly ash, *Sci. Total Environ.*, 407 (2009) 5780–5786.
- [50] M. Macedo-Miranda, M. Olguin, Arsenic sorption by modified clinoptilolite-heulandite rich tuffs, *J. Inclusion Phenom. Macrocyclic Chem.*, 59 (2007) 131–142.
- [51] C.-S. Jeon, K. Baek, J.-K. Park, Y.-K. Oh, S.-D. Lee, Adsorption characteristics of As(V) on iron-coated zeolite, *J. Hazard. Mater.*, 163 (2009) 804–808.
- [52] X. Liu, H. Ao, X. Xiong, J. Xiao, J. Liu, Arsenic removal from water by iron-modified bamboo charcoal, *Water Air Soil Pollut.*, 223 (2012) 1033–1044.
- [53] H.L. Rahman, H. Erdem, M. Sahin, M. Erdem, Iron-incorporated activated carbon synthesis from biomass mixture for enhanced arsenic adsorption, *Water Air Soil Pollut.*, 231 (2020) 6.

- [54] T.G. Asere, S. Mincke, J. De Clercq, K. Verbeke, D.A. Tessema, F. Fufa, C.V. Stevens, G. Du Laing, Removal of arsenic(V) from aqueous solutions using chitosan–red scoria and chitosan–pumice blends, *Int. J. Environ. Res. Public Health*, 14 (2017) 895.
- [55] S. Goldberg, Chemical modeling of anion competition on goethite using the constant capacitance model, *Soil Sci. Soc. Am. J.*, 49 (1985) 851–856.
- [56] M. Mkandawire, Y.V. Lyubun, P.V. Kosterin, E.G. Dudel, Toxicity of arsenic species to *Lemma gibba* L. and the influence of phosphate on arsenic bioavailability, *Environ. Toxicol.*, 19 (2004) 26–34.
- [57] M.A. Rahman, H. Hasegawa, K. Ueda, T. Maki, M.M. Rahman, Arsenic uptake by aquatic macrophyte *Spirodela polyrhiza* L.: interactions with phosphate and iron, *J. Hazard. Mater.*, 160 (2008) 356–361.
- [58] X. Meng, S. Bang, G.P. Korfiatis, Effects of silicate, sulfate, and carbonate on arsenic removal by ferric chloride, *Water Res.*, 34 (2000) 1255–1261.
- [59] S. Ahmadi, C.A. Igwegbe, Adsorptive removal of phenol and aniline by modified bentonite: adsorption isotherm and kinetics study, *Appl. Water Sci.*, 8 (2018) 170.
- [60] S. Ahmadi, A. Banach, F.K. Mostafapour, D. Balarak, Study survey of cupric oxide nanoparticles in removal efficiency of ciprofloxacin antibiotic from aqueous solution: adsorption isotherm study, *Desal. Water Treat.*, 89 (2017) 297–303.
- [61] A.O. Dada, A.P. Olalekan, A.M. Olatunya, O. Dada, Langmuir, Freundlich, Temkin and Dubinin–Radushkevich isotherms studies of equilibrium sorption of Zn²⁺ unto phosphoric acid modified rice husk, *IOSR J. Appl. Chem.*, 3 (2012) 38–45.
- [62] N.K. Mondal, R. Bhaumik, T. Baur, B. Das, P. Roy, J.K. Datta, Studies on defluoridation of water by tea ash: an unconventional biosorbent, *Chem. Sci. Trans.*, 1 (2012) 239–256.
- [63] M. Chiban, G. Carja, G. Lehutu, F. Sinan, Equilibrium and thermodynamic studies for the removal of As(V) ions from aqueous solution using dried plants as adsorbents, *Arabian J. Chem.*, 9 (2016) S988–S999.
- [64] P.S. Blanes, M.E. Bordoni, J.C. González, S.I. García, A.M. Atria, L.F. Sala, S.E. Bellú, Application of soy hull biomass in removal of Cr(VI) from contaminated waters: kinetic, thermodynamic and continuous sorption studies, *J. Environ. Chem. Eng.*, 4 (2016) 516–526.
- [65] S.S. Bagali, B.S. Gowrishankar, A.S. Roy, Optimization, kinetics, and equilibrium studies on the removal of lead(II) from an aqueous solution using banana pseudostem as an adsorbent, *Engineering*, 3 (2017) 409–415.
- [66] S. Ghorai, K. Pant, Equilibrium, kinetics and breakthrough studies for adsorption of fluoride on activated alumina, *Sep. Purif. Technol.*, 42 (2005) 265–271.
- [67] L. Liu, S. Fan, Y. Li, Removal Behavior of Methylene blue from aqueous solution by tea waste: kinetics, isotherms and mechanism, *Int. J. Environ. Res. Public Health*, 15 (2018) 1321.
- [68] T. Sumathi, G. Alagumuthu, Adsorption studies for arsenic removal using activated *Moringa oleifera*, *Int. J. Chem. Eng.*, 2014 (2014) 6.
- [69] E. Bazrafshan, F. Kord Mostafapour, S. Rahdar, A.H. Mahvi, Equilibrium and thermodynamics studies for decolorization of Reactive black 5 (RB5) by adsorption onto MWCNTs, *Desal. Water Treat.*, 54 (2015) 2241–2251.
- [70] V.K. Gupta, Equilibrium uptake, sorption dynamics, process development, and column operations for the removal of copper and nickel from aqueous solution and wastewater using activated slag, a low-cost adsorbent, *Ind. Eng. Chem. Res.*, 37 (1998) 192–202.
- [71] N. Teutscherova, J. Houška, M. Navas, A. Masaguer, M. Benito, E. Vazquez, Leaching of ammonium and nitrate from acrisol and calcsol amended with holm oak biochar: a column study, *Geoderma*, 323 (2018) 136–145.
- [72] P. Singh, S.K. Singh, J. Bajpai, A.K. Bajpai, R.B. Shrivastava, Iron crosslinked alginate as novel nanosorbents for removal of arsenic ions and bacteriological contamination from water, *J. Mater. Res. Technol.*, 3 (2014) 195–202.
- [73] K. Vijayaraghavan, J. Jegan, K. Palanivelu, M. Velan, Batch and column removal of copper from aqueous solution using a brown marine alga *Turbinaria ornata*, *Chem. Eng. J.*, 106 (2005) 177–184.
- [74] P.V. Nidheesh, R. Gandhimathi, S.T. Ramesh, T.S.A. Singh, Adsorption and desorption characteristics of crystal violet in bottom ash column, *J. Urban Environ. Eng.*, 6 (2012) 18–29.
- [75] A. Ahmad, B. Hameed, Fixed-bed adsorption of reactive azo dye onto granular activated carbon prepared from waste, *J. Hazard. Mater.*, 175 (2010) 298–303.
- [76] S. Ghorai, K. Pant, Investigations on the column performance of fluoride adsorption by activated alumina in a fixed-bed, *Chem. Eng. J.*, 98 (2004) 165–173.
- [77] J. Goel, K. Kadirvelu, C. Rajagopal, V.K. Garg, Removal of lead(II) by adsorption using treated granular activated carbon: batch and column studies, *J. Hazard. Mater.*, 125 (2005) 211–220.
- [78] H. Zeng, M. Arashiro, D.E. Giammar, Effects of water chemistry and flow rate on arsenate removal by adsorption to an iron oxide-based sorbent, *Water Res.*, 42 (2008) 4629–4636.
- [79] G. Ayoub, M. Mehawej, Adsorption of arsenate on untreated dolomite powder, *J. Hazard. Mater.*, 148 (2007) 259–266.
- [80] T. Padmesh, K. Vijayaraghavan, G. Sekaran, M. Velan, Biosorption of Acid blue 15 using fresh water macroalga *Azolla filiculoides*: batch and column studies, *Dyes Pigm.*, 71 (2006) 77–82.
- [81] I. Tan, A. Ahmad, B. Hameed, Adsorption of basic dye using activated carbon prepared from oil palm shell: batch and fixed bed studies, *Desalination*, 225 (2008) 13–28.
- [82] Z. Asif, Z. Chen, Removal of arsenic from drinking water using rice husk, *Appl. Water Sci.*, 7 (2017) 1449–1458.
- [83] Z. Aksu, F. Gönen, Biosorption of phenol by immobilized activated sludge in a continuous packed bed: prediction of breakthrough curves, *Process Biochem.*, 39 (2004) 599–613.
- [84] T. Padmesh, K. Vijayaraghavan, G. Sekaran, M. Velan, Batch and column studies on biosorption of acid dyes on fresh water macro alga *Azolla filiculoides*, *J. Hazard. Mater.*, 125 (2005) 121–129.
- [85] H. Patel, Fixed-bed column adsorption study: a comprehensive review, *Appl. Water Sci.*, 9 (2019) 45.
- [86] R. Senthilkumar, D. Reddy Prasad, L. Govindarajan, K. Saravanakumar, B. Naveen Prasad, Synthesis of green marine algal-based biochar for remediation of arsenic(V) from contaminated waters in batch and column mode of operation, *Int. J. Phytorem.*, 22 (2020) 279–286.
- [87] P.T.T. Nguyen, Y. Sanou, S. Pare, H.M. Bui, Removal of arsenic from groundwater using Lamdong laterite as a natural adsorbent, *Pol. J. Environ. Stud.*, 29 (2020) 1305–1314.
- [88] M.N. Haque, G. Morrison, G. Ferrusquia, M. Gutierrez, A. Aguilera, I. Cano-Aguilera, J. Gardea-Torresdey, Characteristics of arsenic adsorption to sorghum biomass, *J. Hazard. Mater.*, 145 (2007) 30–35.
- [89] C.-C. Chen, Y.-C. Chung, Arsenic removal using a biopolymer chitosan sorbent, *J. Environ. Sci. Health, Part A*, 41 (2006) 645–658.
- [90] S. Kundu, A. Gupta, As(III) removal from aqueous medium in fixed bed using iron oxide-coated cement (IOCC): experimental and modeling studies, *Chem. Eng. J.*, 129 (2007) 123–131.
- [91] S. Thanawatpooantawee, A. Imyim, N. Praphairaksit, Iron-loaded zein beads as a biocompatible adsorbent for arsenic(V) removal, *J. Ind. Eng. Chem.*, 43 (2016) 127–132.
- [92] Y. Li, Y. Zhu, Z. Zhu, X. Zhang, D. Wang, L. Xie, Fixed-bed column adsorption of arsenic(V) by porous composite of magnetite/hematite/carbon with eucalyptus wood microstructure, *J. Environ. Eng. Landscape Manage.*, 26 (2018) 38–56.
- [93] H.N. Nhat Ha, N.T. Kim Phuong, T. Boi An, N.T. Mai Tho, T. Ngoc Thang, B. Quang Minh, C. Van Du, Arsenate removal by layered double hydroxides embedded into spherical polymer beads: batch and column studies, *J. Environ. Sci. Health, Part A Toxic/Hazard. Subst. Environ. Eng.*, 51 (2016) 403–413.